Supplemental Material

A digital sensor to measure real-time leaf movements and detect abiotic stress in plants

Geldhof Batist, Pattyn Jolien, Eyland David, Carpentier Sebastien, Van de Poel Bram

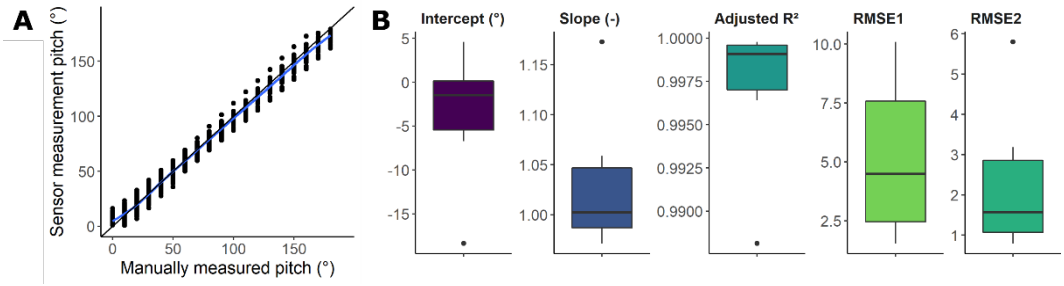

Supplemental Figure S1: Sensor calibration and accuracy. (A) Angle values of 64 sensors for the pitch (θ) orientation, calibrated against manual angle measurements using a protractor system. The RMSE of a single linear model fit through all data points was 4.9°. (B) Boxplot representation of intercept, slope and adjusted R^2 for Individual sensor-specific linear models (center line = median, box limits = first and third quartile, whiskers = largest and smallest value within 1.5 x interquartile range, individual points = outliers). RMSE1 was determined for the sensor-to-angle differences and RMSE2 for the deviation of the individual sensor models from the ground truth.

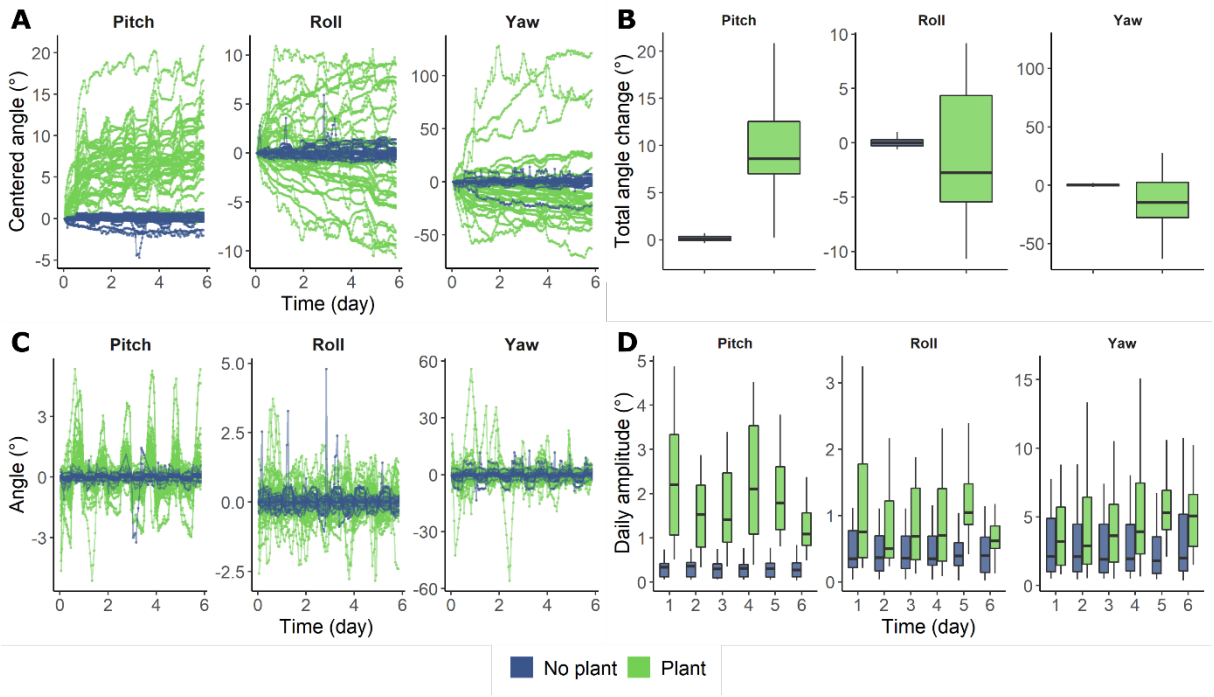

Supplemental Figure S2: Comparison of steady-state sensor behavior to plant movements. (A) Sensor stability of individual sensors for 6 days in steady-state conditions (not attached to a plant leaf) in blue (n = 35) as compared to actual angular changes of individual sensors attached to banana leaves in green (n = 25) for the pitch (θ), roll (φ) and yaw (ψ) movement. (B) Boxplots showing total angle change for the pitch, roll and yaw movement over 6 days for the sensors in steady state and the sensors attached to a banana leaf (center line = median, box limits = first and third quartile, whiskers = largest and smallest value within 1.5 x interquartile range). (C) Seasonal trend (daily oscillations) of sensors in steady state (blue) and attached to a banana leaf (green) and (D) their daily amplitudes, for the pitch (θ), roll (φ) and yaw (ψ) movement.

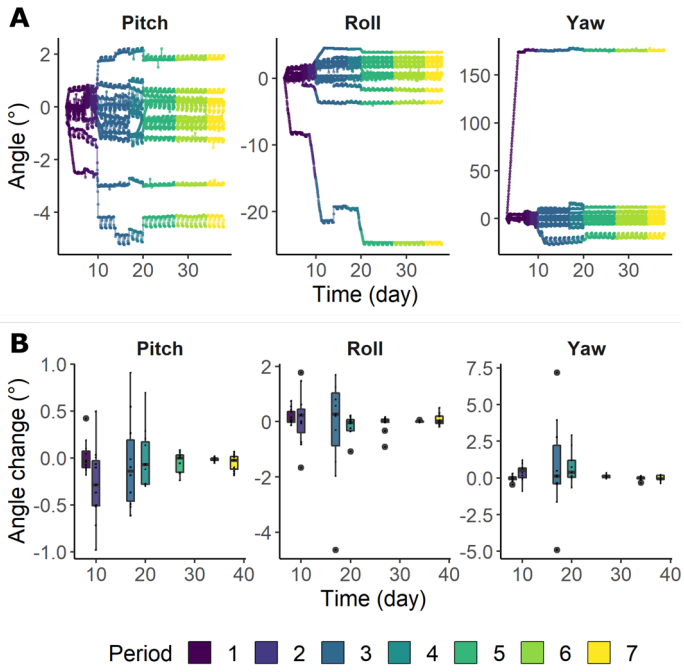

Supplemental Figure S3: Long-term steady-state sensor stability. (A) Angle data of 12 individual IMU sensors for a period of 34 days for the pitch (θ), roll (φ) and yaw (ψ) movement. Each color represents a period of undisturbed measurements. The last 14 days of the sequence, there were no intermittent experiments. (B) Boxplots of the total change of angular orientation within the 34 day measurement period (center line = median, box limits = first and third quartile, whiskers = largest and smallest value within 1.5 x interquartile range, individual points = outliers). Each boxplot represents the change of the angle during a period of undisturbed measurements.

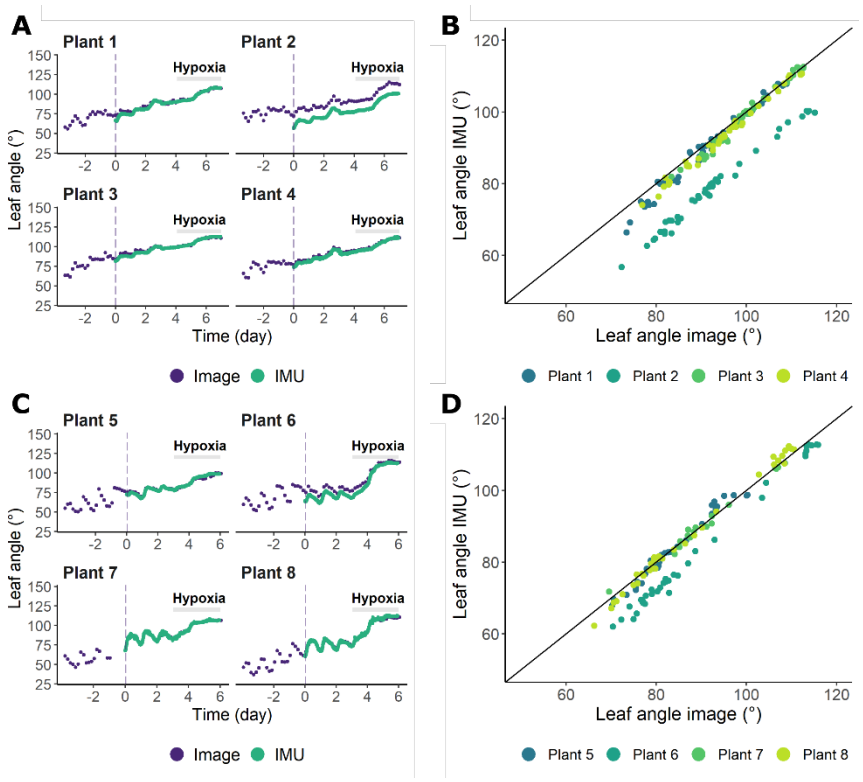

34

35 Supplemental Figure S4: Validation of the sensor pitch movement before and during root hypoxia for tomato (Ailsa Craig). Eight
36 plants were monitored during two subsequent imaging periods. (A & C) Time series comparison between image-based leaf
37 angle measurements and IMU sensor output. Leaf petioles were first imaged for several days prior to the attachment of the
38 IMU sensor to the leaf petiole, to assess the effect of the sensor weight on the leaf movement. The dashed line in (A & C)
39 indicates the start of the sensor measurement. (B & D) Correlation between the petiole angle derived from image analysis and
40 the leaf angle sensors (mean R^2_{adj} = 0.987 ± 0.007 and mean RMSE = 3.92° ± 4.38°).

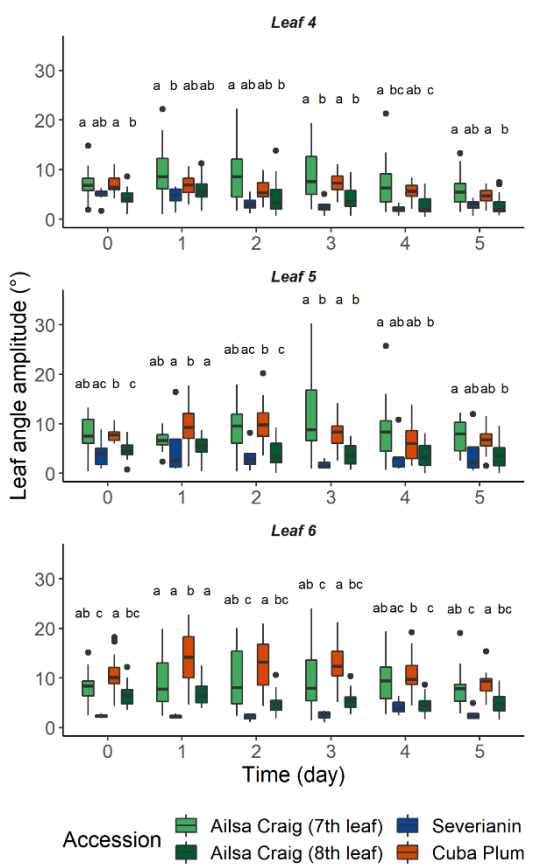

Supplemental Figure S5: Leaf angle amplitudes of the circadian rhythms of leaves of different ages and different tomato accessions. Amplitudes of the pitch movement are shown for leaf 4, 5 and 6 of Ailsa Craig tomato plants of different plant ages (7 and 8 leaves on average), and of two other distinct tomato accessions (Severianin and Cuba Plum) for 5 days (n = 10). The amplitude was calculated as the daily change of the leaf oscillation, excluding the long-term trend (center line = median, box limits = first and third quartile, whiskers = largest and smallest value within 1.5 x interquartile range, individual points = outliers). Significant differences between the treatments were determined using a non-parametric Dunn's test with Bonferroni correction ($\alpha = 0.05$) and are represented by different letter codes.

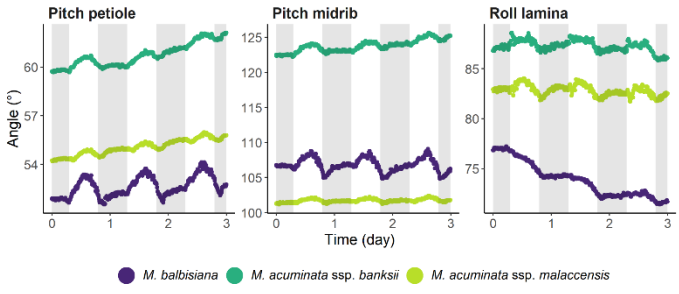

Supplemental Figure S6: Non-centered data of the circadian leaf movements of different banana genotypes (corresponding to Figure 3C).. Circadian rhythms of the pitch movement of the leaf petiole and midrib and the roll movement of the leaf lamina in a single leaf of three banana genotypes (*Musa balbisiana*, *Musa acuminata* ssp. *banksii* and *Musa acuminata* ssp. *malaccensis*).

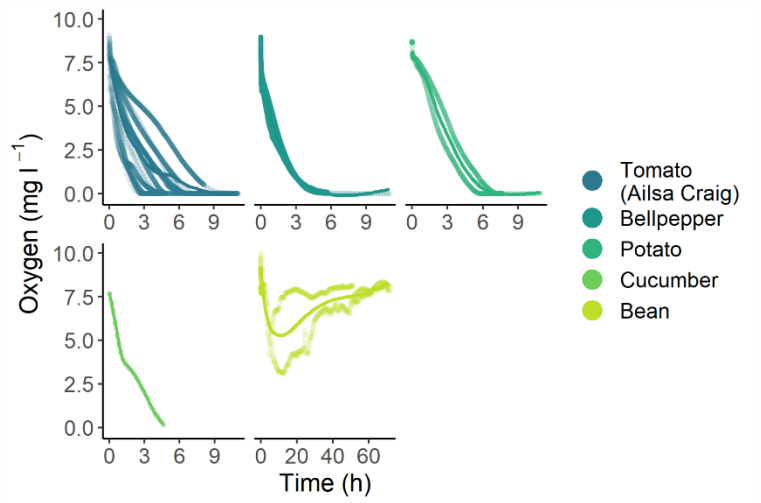

Supplemental Figure S7: Oxygen consumption in the root zone of individual plants of different species during a waterlogging treatment. Lines represent the smoothed model on the raw data.

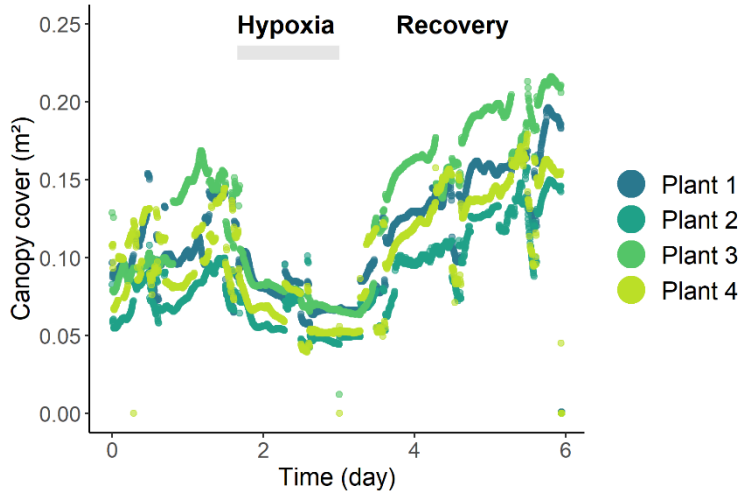

Supplemental Figure S8: Real-time canopy cover change in Ailsa Craig tomato plants during waterlogging. Data were collected for 4 plants (n = 4) during a waterlogging treatment of 32h and the subsequent reoxygenation. Canopy cover was derived as the projected leaf surface from top-view images.

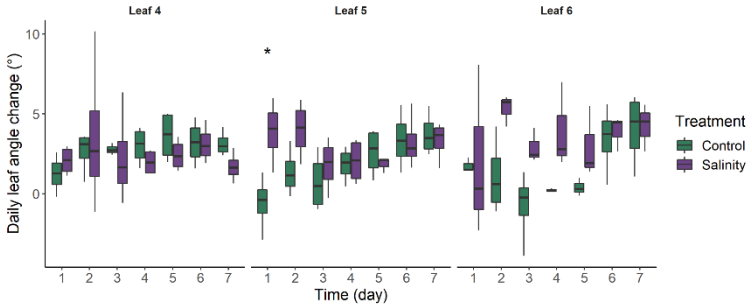

Supplemental Figure S9: Average daily leaf angle trend change during control and high salinity conditions in tomato (cv. Ailsa Craig) (n = 4, EC = 10). Daily leaf angle change is expressed as the difference between subsequent mean daily angles (center line = median, box limits = first and third quartile, whiskers = largest and smallest value within 1.5 x interquartile range, individual points = outliers). Significant differences between the treatments were determined using a non-parametric Wilcoxon test (α = 0.05) and are indicated with an asterisk (*).

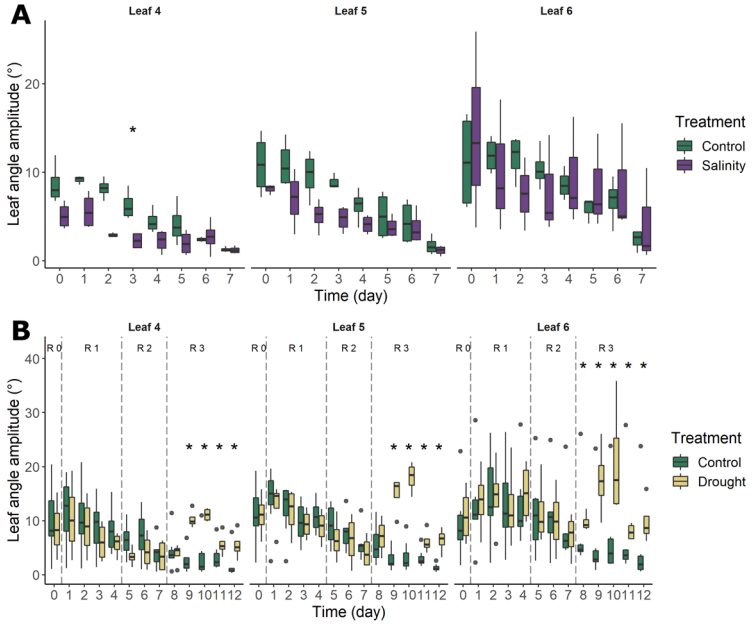

Supplemental Figure S10: Daily leaf angle amplitudes of leaves of different ages (4th, 5th and 6th leaf) during abiotic stress conditions in tomato (cv. Ailsa Craig). The amplitude was calculated as the daily change of the leaf oscillation, excluding the long-term trend (center line = median, box limits = first and third quartile, whiskers = largest and smallest value within 1.5 x interquartile range, individual points = outliers). (A) Salt treatment with sodium chloride enriched irrigation for seven days (n = 4; EC = 10); (B) Drought treatment with decreasing watering regimes: R0 = well-watered; R1 = irrigation in the morning and the evening; R2 = irrigation in the morning; R3 = no irrigation (n = 4 – 8). Significant differences between the treatments were determined using a non-parametric Wilcoxon test (α = 0.05) and are indicated with an asterisk (*).

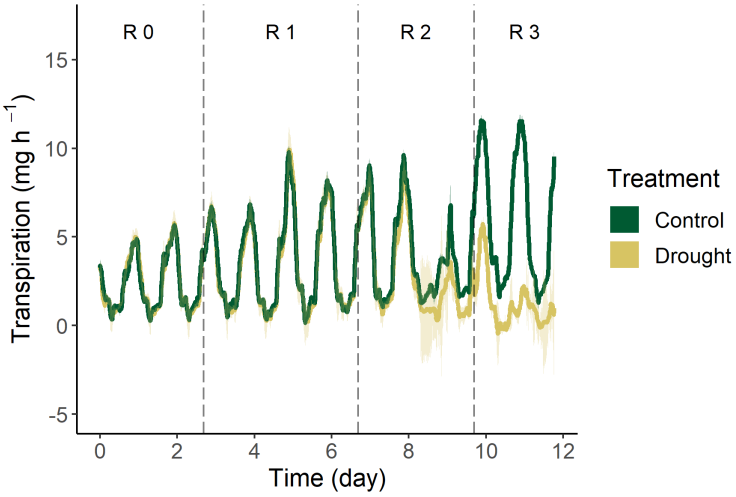

Supplemental Figure S11: Mean hourly transpiration of tomato (cv. Ailsa Craig) plants during well-watered conditions and drought stress, together with the 90 % confidence interval. The drought sequence consisted of 4 regimes (R0 = well-watered; R1 = irrigation in the morning and the evening; R2 = irrigation only in the morning; R3 = no irrigation).

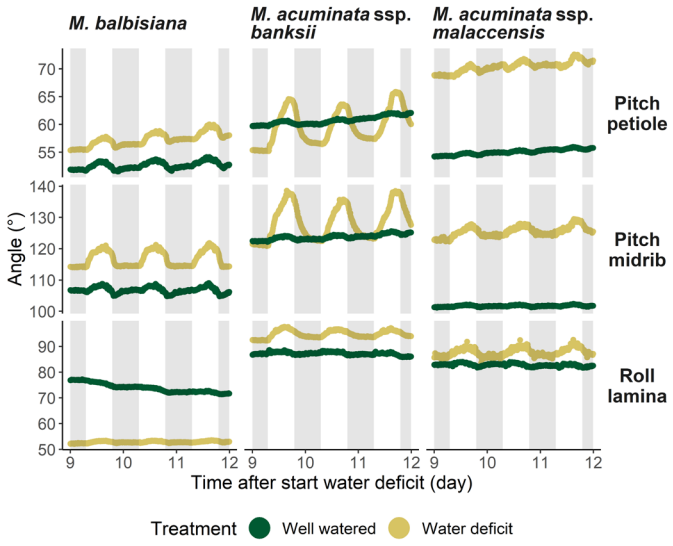

Supplemental Figure S12: Non-centered data of the circadian leaf movements of banana during drought stress (corresponding to Figure 5C). Comparison of the leaf orientation of the petiole, midrib and lamina of a single leaf between three banana genotypes (*Musa balbisiana*, *Musa acuminata* ssp. *banksii* and *Musa acuminata* ssp. *malaccensis*) in well-watered (green) and water deficit (yellow) conditions.

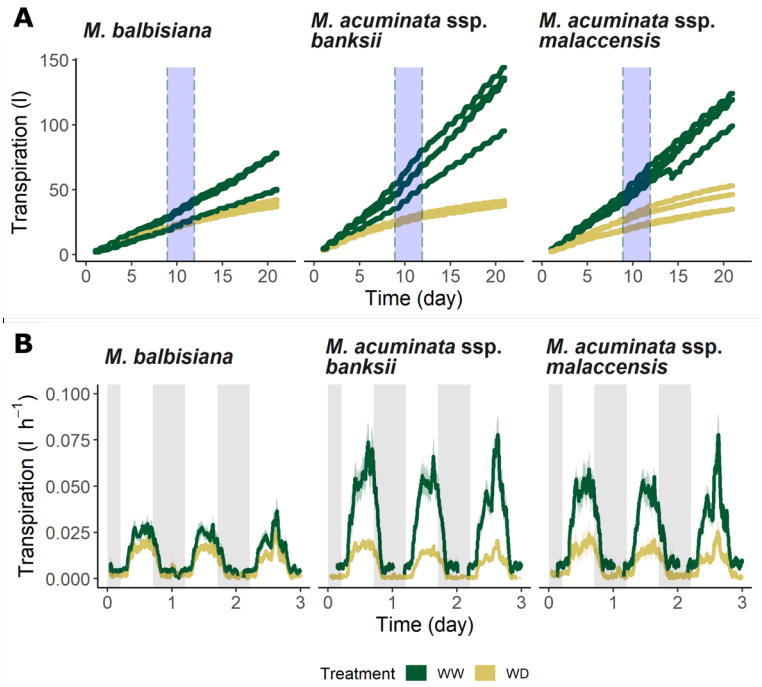

Supplemental Figure S13: Transpiration of three banana genotypes during well-watered and water deficit conditions. (A) Cumulative transpiration for the total duration of the experiment for the three banana genotypes (*Musa balbisiana*, *Musa acuminata* ssp. *banksii* and *Musa acuminata* ssp. *malaccensis*) during well-watered and water deficit conditions (n = 4). The shaded region between dashed lines corresponds to the three-day period of leaf angle measurements. (B) Mean hourly transpiration of the three banana genotypes during well-watered and water deficit conditions, together with the 90 % confidence interval (n = 4). This three day period corresponds to the timeframe of leaf angle measurements presented in Figure 5.

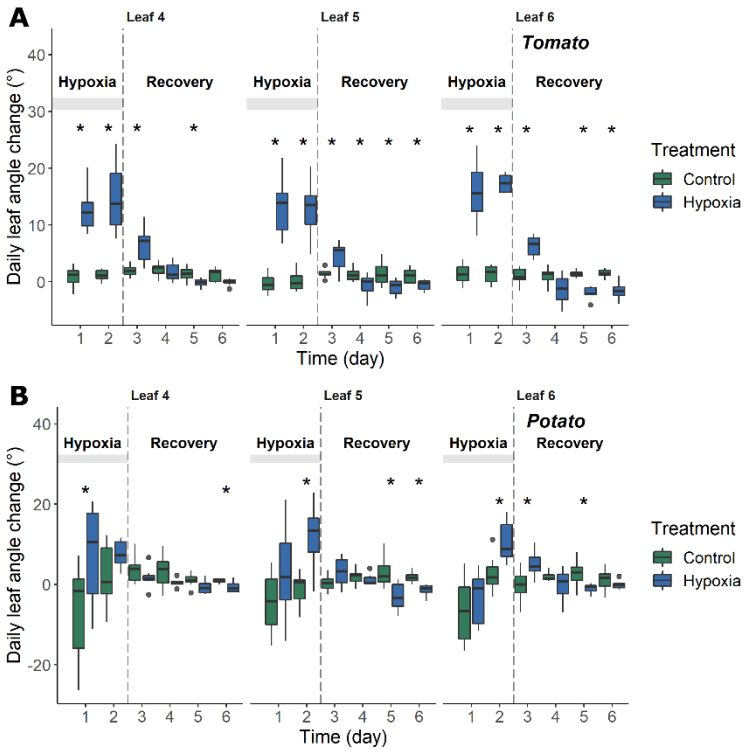

Supplemental Figure S14: Comparison of the daily leaf angle changes during waterlogging of tomato and potato. (A) Leaves of different ages (4th, 5th and 6th leaf) of tomato (cv. Ailsa Craig) (n = 10) and (B) leaves of different ages (9th, 10th and 10th leaf) of potato (n = 9). Daily leaf angle change is expressed as the difference between subsequent mean daily angles (center line = median, box limits = first and third quartile, whiskers = largest and smallest value within 1.5 x interquartile range, individual points = outliers). Significant differences between the treatments were determined using a non-parametric Wilcoxon test (α = 0.05) and are indicated with an asterisk (*).

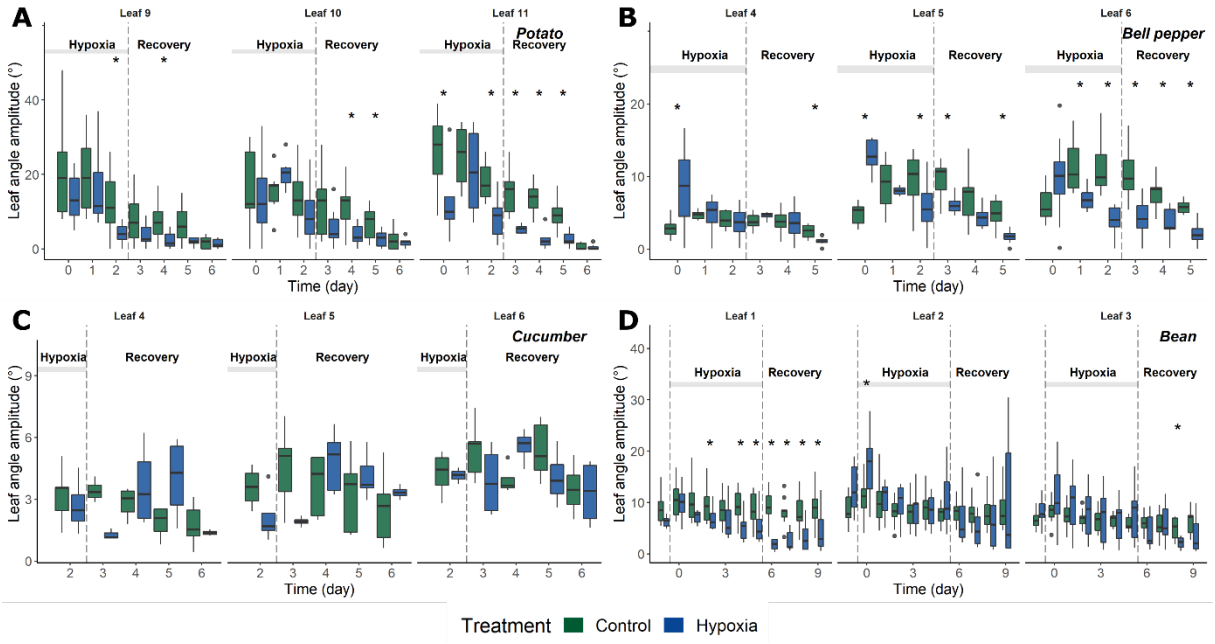

Supplemental Figure S15: Daily leaf angle amplitudes of different aged leaves and in different species during a waterlogging treatment and recovery. The amplitude was calculated as the daily change of the leaf oscillation, excluding the long-term trend (center line = median, box limits = first and third quartile, whiskers = largest and smallest value within 1.5 x interquartile range, individual points = outliers). The amplitude of the daily leaf angle is depicted for (A) potato leaves of different ages (4th, 5th and 6th leaf) (n = 9); (B) bell pepper leaves of different ages (4th, 5th and 6th leaf) (n = 10); (C) cucumber leaves of different ages (4th, 5th and 6th leaf) (n = 5) and (D) bean leaves of different ages 1th, 2nd and 3th leaf) (n = 10). Significant differences between the treatments were determined using a non-parametric Wilcoxon test ($\alpha = 0.05$) and are indicated with an asterisk (*).

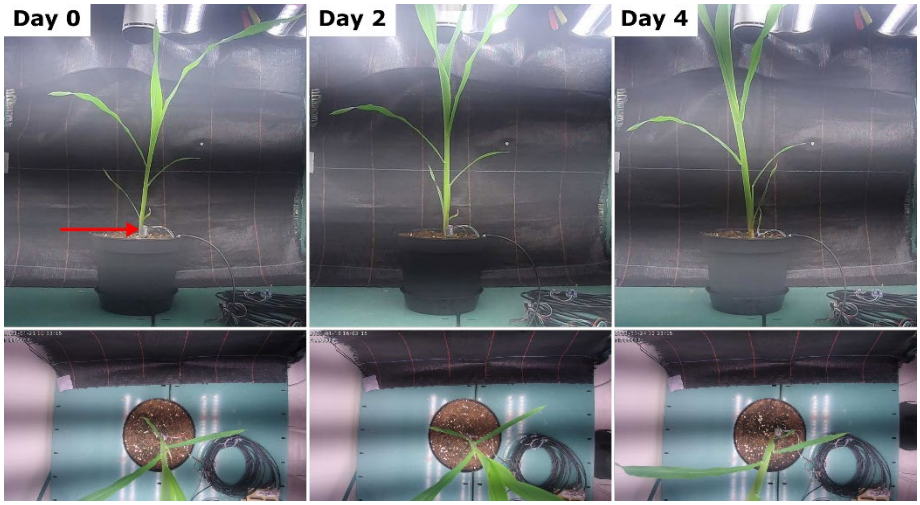

Supplemental Figure S16: Side- and top-view images of the orientation of a single maize plant during 4 days of growth. The sensor was attached to the stem base (red arrow). The maize plant depicted here corresponds to the plant on which stem angle measurements were performed (Figure 8).